Molecular Crystals and Liquid Crystals Science and Technology. Section A. Molecular Crystals and Liquid Crystals
Publication details, including instructions for authors and subscription information:
http://www.tandfonline.com/loi/gmcl19

Electro-Optical and Morphological Characterization of Electron Beam Cured Liquid Crystal-Polymer Composite Materials

U. Maschke [a] , J.-M. Gloaguen [b] , J.-D. Turgis [a] & X. Coqueret [a]
[a] Laboratoire de Chimie Macromoléculaire, CNRS (URA N°351)
[b] Laboratoire de Structure et Propriétés de l'Etat Solide, CNRS (URA N°234) Université des Sciences et Technologies de Lille, 59655, Villeneuve d'Ascq, France
Version of record first published: 24 Sep 2006.

To cite this article: U. Maschke , J.-M. Gloaguen , J.-D. Turgis & X. Coqueret (1996): Electro-Optical and Morphological Characterization of Electron Beam Cured Liquid Crystal-Polymer Composite Materials, Molecular Crystals and Liquid Crystals Science and Technology. Section A. Molecular Crystals and Liquid Crystals, 282:1, 407-417

To link to this article: http://dx.doi.org/10.1080/10587259608037594

Mol. Cryst. Liq. Cryst., 1996, Vol. 282, pp. 407–417
Reprints available directly from the publisher
Photocopying permitted by license only

ELECTRO-OPTICAL AND MORPHOLOGICAL CHARACTERIZATION OF ELECTRON BEAM CURED LIQUID CRYSTAL-POLYMER COMPOSITE MATERIALS

U. MASCHKE, J.-M. GLOAGUEN[+], J.-D. TURGIS AND X. COQUERET
Laboratoire de Chimie Macromoléculaire, CNRS (URA N°351)
[+] Laboratoire de Structure et Propriétés de l'Etat Solide, CNRS (URA N°234)
Université des Sciences et Technologies de Lille, 59655 Villeneuve d'Ascq, France

Abstract
Polymer dispersed liquid crystals (PDLCs) are promising new materials for electro-optic applications such as switchable windows and flexible displays. Thin films were prepared via a polymerization induced phase separation process using electron beam radiation. The PDLC material was obtained from a blend of a eutectic nematic liquid crystal mixture E7 and a polyester acrylate based polymer as a precursor of the matrix. The electro-optic behavior of the obtained composite material has been examined. To understand the optical response of these materials, the relationship between the electro-optic properties and the morphology of the PDLC films has been investigated. The size, size distribution, shape, volumetric number density and spatial distribution of droplets are important factors influencing the electro-optic performance. Scanning electron microscopy (SEM) was used to characterize quantitatively PDLC film morphology.

INTRODUCTION

Polymer dispersed liquid crystal (PDLC) films are composite materials consisting of low molecular weight liquid crystals dispersed as micron sized droplets in a solid polymer matrix.[1,2] These materials are of considerable interest as novel materials for display applications and light shutter devices. Polymerization induced phase separation (PIPS) initiated by electron beam (EB) radiation is proved to be a powerful method to obtain well defined PDLC films.[3-5] Electron beam processing offers various advantages : high conversion of monomers, controlled degree of crosslinking, fast cure rate, no need for thermal activation. Compared with the PIPS process by ultraviolet light,[6] electron beam curing results in completely crosslinked polymer matrices without the use of any initiating compound.

The principle of operation is based on the electric field controlled transmission properties of the composite material sandwiched between two transparent conducting electrodes. Light is efficiently scattered in the initial off-state essentially because of the birefringence of the liquid crystals and the refractive index differences between the liquid crystal in the droplets and the polymer matrix. The nematic liquid crystals used in the experiments exhibit positive dielectric anisotropy at low frequencies and therefore align with their optical axis parallel to an externally applied electrical field. In the on-state, light incident normal to the film surface probes essentially the ordinary refractive index n_o of the liquid crystals. The film appears transparent if the refractive index of the matrix approximately matches n_o. Upon removal of the voltage, the droplets return to their original random orientation that induces light scattering.

The electro-optic properties of PDLC films are influenced by several factors including film thickness, liquid crystal droplet size and shape, droplet director configuration, distribution of droplets in size, shape and in space, volume fraction of droplets. These parameters are determined primarily by the phase separation process and the curing kinetics depending on the initial reactive mixture. The electro-optic characteristics also depend on the choice of the wavelength of detection, the driving frequency, the angle of observation and the applied voltage as a function of time. All steps mentioned above might be also temperature controlled.

In this paper, the relationship between the electro-optic properties and the morphology of PDLC films based on one selected representative composition has been examined. Scanning electron microscopy (SEM) was applied to characterize quantitatively the morphology of the composite materials. Binary images were created from the obtained SEM micrographs. The use of two different image treating programs and two different techniques for sample preparation allow to obtain detailed and comparable informations about the microstructure. The results of this analysis enable to calculate the effective refractive index of the polymer matrix and to estimate the scattering cross section of a liquid crystal droplet.

EXPERIMENTAL

Materials

The liquid crystal mixture E7 (Merck Ltd, GB) was used during this work; it exhibits the following refractive indices at 20°C: n_o=1.5183, n_e=1.7378 (λ=632.8 nm).[7] The prepolymer chosen consists of an aromatic polyester acrylate (Rahn AG, Switzerland) diluted in additional monomers including Tripropyleneglycoldiacrylate (UCB, Belgium). The refractive index of the prepolymer in the cured state in the absence of E7 is

n_p=1.5120 (λ=632.8 nm).[8]

Preparation of PDLC films

The prepolymer and the liquid crystals were mixed together at room temperature in the ratio 1:1 by weight until the mixture became homogeneous. The thickness and the uniform application of the liquid mixture on flat microscopic glass plates was controlled by using a wire wound rod as a bar-coater or a leveling blade device. A bar-coater of 25μm (Braive, Belgium) allowed to prepare the sample series 1 that was also used for electro-optical characterization. The sample series 2 was obtained by means of a blade device which results in a more uniform liquid film. For each series, several samples have been prepared and exposed to the electron beam irradiation to cure the polymerizable composition.

The glass plates used for the electro-optic experiments were coated with a thin transparent layer of conducting indium-tin-oxide (ITO) (Balzers, Liechtenstein). Samples prepared for SEM studies were kept under reduced pressure (P=0.1 Torr) at a temperature of 40°C. The loss of E7 by evaporation is high enough to consider that the film surface is liberated of liquid crystals.

Electron beam curing

The electron beam generator used to prepare the PDLC samples by a PIPS process was an Electrocurtain Model CB 150 (Energy Sciences Inc.) with an operating high voltage of 175 kV. The glass plates were placed in a sample tray, which was passed under an inert atmosphere (oxygen content typically between 130 and 160 ppm for the present irradiations) to the accelerated electron curtain on a conveyor belt. The applied dose of 60 kGy was achieved by using a beam current of 4 mA and a conveyor speed of 0.22m/s. These values have not been changed during our experiments in order to apply each time the same curing conditions. Since the film thickness did not exceed 50 μm, the applied dose was delivered in an uniform way in the depth of the sample. No temperature control during the irradiation process has been performed.

Film thicknesses were deduced from a micrometer calliper (Mitutoyo; uncertainty: ± 1μm). To minimize errors in the determination of film thickness, eighteen different places on each plate before and after composite film preparation were taken into account.

Electro-optic measurements

The electro-optic experiments were carried out at room temperature using a Cary 219 spectrophotometer (Varian Associates) at a wavelength of λ=625 nm with a bandwidth of 3 nm using a driving AC of frequency 140 Hz. The cured PDLC films on the glass

plates were sandwiched by another ITO coated glass substrate.

The transmission properties of the PDLC-cells were measured by passing the light through the cells normal to the film surface. The transmitted intensity has been corrected from the loss of transparency which results from the reversible darkening of the glass plates upon EB irradiation.

Starting from the electrical off-state, the applied voltage was increased in steps of five volts with a step time of one minute until a further increase of voltage did not vary the transmission values. After the first scan up cycle, the voltage was decreased in the same way before the whole procedure was twice repeated. Between two complete cycles, the cells were kept for a period of five minutes in the field-off state.

SEM measurements

Quantitative characterization of droplet sizes by SEM can be performed by analyzing undistorted top views of PDLC samples. The sample preparation technique as described above reveal the droplets as empty cavities that were once filled with liquid crystals. The PDLC samples were characterized by means of a scanning electron microscope (Cambridge Instrument 250) using secondary electrons. Prior to observation, SEM samples were coated with gold (thickness 20-30 nm) in order to provide an electrically conductive layer, to suppress surface charges, to minimize radiation damage and to increase electron emission. The magnification used in our experiments was about 1500x using an acceleration voltage of 10kV. The range of the analysis was situated in a depth of approximately 0.5 μm from the film surface. 256 grey level images at a resolution of 72 DPI (Dots per inch) were subsequently stored on the hard disk for further analysis. The obtained images have been analyzed by using two different software programs called ESILAB (produced by Desy and distributed by Newtec) and NIH - IMAGE. The first step to characterize quantitatively the microstructure was to generate binary images i.e. images in which the pixels are either turned on or off. In the case of data treatment by ESILAB, this has been done after calibration (pixels-microns) and definition of the working window by using a morphological filtering on the grey level ("Chapeau haut de forme") followed by a threshold operation. The generated binary images have been compared droplet by droplet with the corresponding original SEM micrographs. The binary images were recreated until all droplets revealed the same size and form as in the micrographs. Special emphasis has also been paid to the control of the total number of objects before and after processing.

Based on the same generated binary images, droplet size and shape analysis of the samples of the first series has been carried out by using independently ESILAB- and IMAGE-processing programs.

RESULTS AND DISCUSSION

Film microstructure and data analysis

SEM analysis allows to determine the microstructure of PDLC films and to obtain geometrical quantities related to the droplets like size, shape, surface, perimeter and orientation.[9-11] All samples used in this work exhibited a morphology whereby the liquid crystal is confined to microdroplets dispersed in a continuous polymer matrix. A representative example of the observed microstructure is shown in Figure 1. The cross-sections of the droplets are not interconnected, they do not exhibit a preferred orientation of their major length axis and they are uniformly dispersed within the polymer matrix. The SEM micrographs of the samples of series 1 are also characterized by the presence of parallel straight lines resulting from the application of a bar-coater during the sample preparation. These lines are absent in the micrographs of the samples of the second series due to the application of a blade instead of the wire wound rod. Up to now there is no evidence for any other influence of the sample preparation techniques we used on the PDLC film morphology.

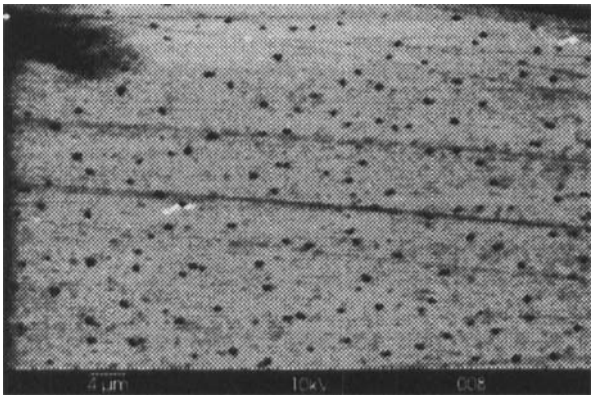

FIGURE 1 Scanning electron micrograph showing a representative top-view of a PDLC film

The obtained PDLC-micrographs were compared with SEM observations of films of the cured polymer to verify that the surface of the polymer film do not exhibit a microstructure similar to that of the PDLC films. It has been shown on several samples that the polymer film surface was completely flat and not distorted.

Some SEM micrographs could not be treated by ESILAB because of a decrease in the grey scale range that reveals the limits of the cavities of the former liquid crystals. This leads to a loss of accuracy in the generation of binary images. For samples of the second series, photos of the original SEM micrographs have been produced on a larger

scale to allow to draw by hand the size and form of all droplets on a transparent paper After careful comparison of the resulting drawing with the original micrograph and scanning of the revealed droplets, the IMAGE processing program was used for droplet size analysis.

All samples in both series exhibited random oriented ellipsoidal cavities presenting monomodal length axis distributions which can be characterized by a single mean length axis in the range of 0.6 μm. The overall range of major length axis values for all samples was between 0.1μm and 1.4 μm. The inset of Figure 2 shows a representative distribution of q-values where q denotes the axial ratio of the length of the minor to the major axis. The results of the data analysis of the droplet cross-sections based on the two sample series using ESILAB and IMAGE processing programs are summarized in Table I, where a_{av}, b_{av} represent the number average of the major, minor length axis and q_{av} the ratio $(b/a)_{av}$. Due to the relatively low resolution (72 DPI) of the original grey level images, careful editing of all a and b values obtained for series 1 revealed the presence of not continuously distributed values. Nevertheless, the results of data analysis for series 2, on the other hand, are comparable with those of series 1 in spite of the higher resolution of the scanned images (120 DPI).

TABLE I Cross-sectional data of liquid crystal droplets in PDLC films

Series, method	a_{av}(μm)	b_{av}(μm)	q_{av}
Series 1 ESILAB	0.58 ± 0.20	0.40 ± 0.14	0.70 ± 0.14
Series 1 IMAGE	0.45 ± 0.15	0.33 ± 0.11	0.74 ± 0.15
Series 2 IMAGE	0.63 ± 0.28	0.46 ± 0.19	0.77 ± 0.16

Since SEM analysis provides information about droplet cross-sections and not about the droplets itself, the obtained data per unit surface have to be converted to unit volume using matrix transformations.[12-14] Since both oblate and prolate ellipsoids produce ellipses on random plane sections, the type of ellipsoid has to be determined. Oblate ellipsoids are present in our case since the size of the largest equiaxed section is comparable to the major axis length of the most unsymmetrical sections. De Hoff's analysis of the size distribution of ellipsoids of revolution from random plane sections can be applied using the following assumptions based on observations made from our two-dimensional data: a) All particles present in the sample can be considered as ellipsoids of revolution b) The ellipses do not exhibit a preferred orientation c) The shape of the ellipsoids is defined by the axial ratio of the generating ellipse d) The area (working window) is large enough to represent the average of all possible random sections. In order to simplify the calculations and due to the fact that a mathematical

equation describing the shape factor k(q) as a function of q was not available, our consideration was limited to the case that all ellipsoids present in the samples were characterized by the same shape factor. The following equation allows to estimate the number of droplets per unit volume in m given size classes

$$N_j = \frac{1}{k(q)\Delta} \sum_{i=j}^{m} n_i \beta_{ji} \qquad (1)$$

where Δ is the bin size of the histogram expressed in μm, n_i the number of ellipses per unit area with major axis length between $(i-1)\Delta$ and $i\Delta$. The coefficients β_{ji} are the results from the solution of the set of m equations and were collected by Saltykov.[15] Nj denotes the number of ellipsoids per unit volume with major length axis between $(j-1)\Delta$ and $j\Delta$. The maximum major axis length for both ellipses and ellipsoids is $m\Delta$.

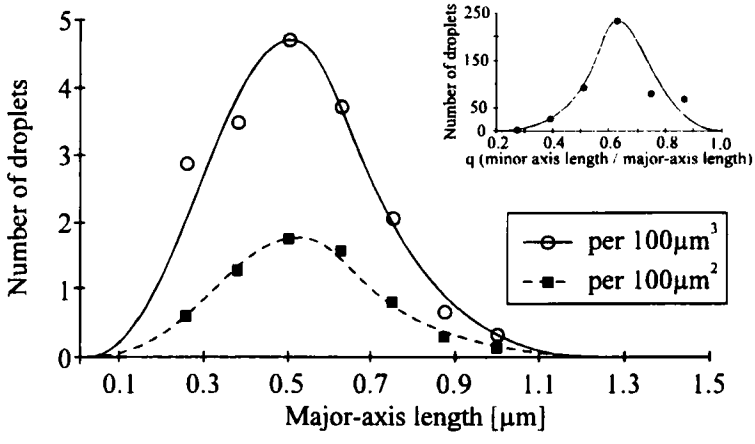

FIGURE 2 Droplet-size distribution per unit area and per unit volume for series 1, ESILAB

Figure 2 shows the droplet size distribution per unit area (cross-sectional data) and per unit volume for series 1 (ESILAB). The open circles and the filled squares in the graph represent the n_i and N_j values for the different size classes as a function of major length axis The lines serve as guidelines for the eyes and are used instead of histograms. Both surface and volume data reveal a nearly monodisperse droplet size distribution exhibiting approximately the same average droplet size. The droplet size distribution per unit volume for series 1 (ESILAB) has been compared in Figure 3 with the corresponding calculations for series 1 (IMAGE) and series 2 (IMAGE). Droplet data analysis performed by IMAGE and ESILAB processing programs on the same binary images do not strictly result in equivalent quantities characterizing the droplets.

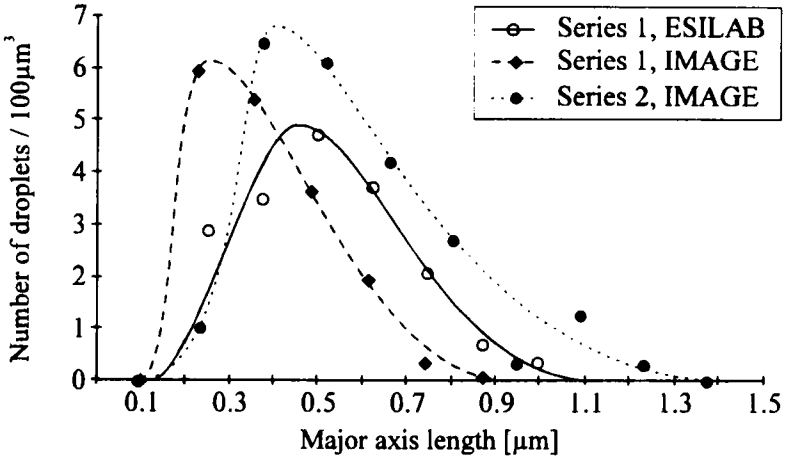

FIGURE 3 Droplet-size distribution per unit volume

Different algorithms might be responsible for this discrepancy. It has been already mentioned above that the low resolution of the generated binary images do not allow precise calculations of droplet sizes of series 1. Regarding the small total interval between the smallest and the largest major length axis obtained during this study, the overal average droplet sizes and droplet size distributions are, however, comparable for all series and processing programs used.

In order to obtain finally the volume fraction α of droplets in the PDLC film, volume calculations based on standard formulas of oblate ellipsoids of revolution have been carried out. The results are gathered in Table II.

Electro-optic behavior

It has been shown that the transmittance characteristics depend strongly on the refractive indices of both the polymer matrix and the droplets.[16-19] A high degree of transparency of PDLC films in the on-state will be only achieved if the refractive index of the polymer matrix is approximately equal to the ordinary refractive index of the liquid crystal. For several reasons the refractive indices of the materials present in PDLC films may differ from the values obtained from independent experiments on pure E7 and the polymer matrix, respectively. In most cases reported so far, the liquid crystal is dissolved partially in the cured polymer matrix, sometimes up to high percentages. The knowledge of the volume fraction of liquid crystals α dissolved in the polymer matrix allow to determine the effective refractive index of the polymer matrix. The calculation was performed using the formalism derived by Montgomery et al.[19]

$$\alpha = \frac{V_{LC}^{matrix}}{V^{matrix}} = \frac{V_{LC}^{matrix}}{V_{polymer}^{matrix} + V_{LC}^{matrix}} = \frac{\beta - \gamma(1+\beta)}{(1-\gamma)(1+\beta)} \quad (2)$$

where V_{LC}^{matrix} represents the volume of liquid crystal dissolved in the polymer matrix and $V_{polymer}^{matrix}$ the volume of the cured polymer. β and γ are given by writing

$$\beta = \frac{V_{LC}}{V_{polymer}^{matrix}} = \frac{V_{LC}^{matrix} + V_{LC}^{droplets}}{V_{polymer}^{matrix}} \quad (3)$$

$$\gamma = \frac{V_{LC}^{droplets}}{V^{total}} = \frac{V_{LC}^{droplets}}{V_{polymer}^{matrix} + V_{polymer}^{droplets} + V_{LC}^{matrix} + V_{LC}^{droplets}} \quad (4)$$

V_{LC} denote the volume occupied by all liquid crystals and $V_{LC}^{droplets}$ represents the volume of liquid crystals in the droplets. It has been checked by FTIR experiments that the remaining monomer/precursor content after the EB curing process was negligible. The volume of residual polymer precursors in the droplets $V_{polymer}^{droplets}$ will be neglected. In this case, the refractive index of the liquid crystal in the droplets n_{LC} can be approximated by taking the average $\langle n_{LC} \rangle^2 = \frac{1}{3}(n_e^2 + 2n_o^2)$. The refractive index of the polymer matrix n_{matrix} is estimated assuming a linear dependence on the volume fraction expressed by :

$$n_{matrix} \approx \gamma \; n_{LC} + (1-\gamma) \; n_p \quad (5)$$

where n_p corresponds to the refractive index of the pure cured polymer matrix. The refractive indices used for the calculations were n_{LC} = 1.5950 and n_p = 1.512. Special emphasis has been paid to the evaluation of the densities of the polymer precursors and of the PDLC films. An average value of 5% volume contraction for the PDLC films was applied to obtain $V_{polymer}^{matrix}$ from $V_{polym\ precursor}$. It was assumed that no change of the total liquid crystal volume occurs during the polymerization process. The density of the polymer precursors was δ = 1.123 and of the liquid crystals δ = 1.0282 (T=25°C)[20]. The scattering cross section of a liquid crystal droplet is proportional to $|s-1|^2$, where $s = n_{matrix}/n_{LC}$. Table II shows the results of the calculations :

TABLE II Influence of the fraction of dissolved liquid crystal on scattering properties

	γ	β	α	n_{matrix}	s	$10^3\|s-1\|^2$
Series 1 ESILAB	0.082	1.15	0.49	1.5527	1.0272	0.742
Series 1 IMAGE	0.035	1.15	0.52	1.5552	1.0256	0.655
Series 2 IMAGE	0.135	1.15	0.46	1.5502	1.0289	0.835

Notes: $\alpha = \frac{V_{LC}^{matrix}}{V^{matrix}}$ $\gamma = \frac{V_{LC}^{droplets}}{V^{total}}$ $\beta = \frac{V_{LC}}{V_{polymer}^{matrix}}$ $s = \frac{n_{matrix}}{n_{LC}}$

In spite of the varying γ-values obtained from data analysis of the SEM micrographs, the effective refractive index of the polymer matrix and hence the scattering efficiency of the PDLC films are comparable independent of the sample series and data treatment

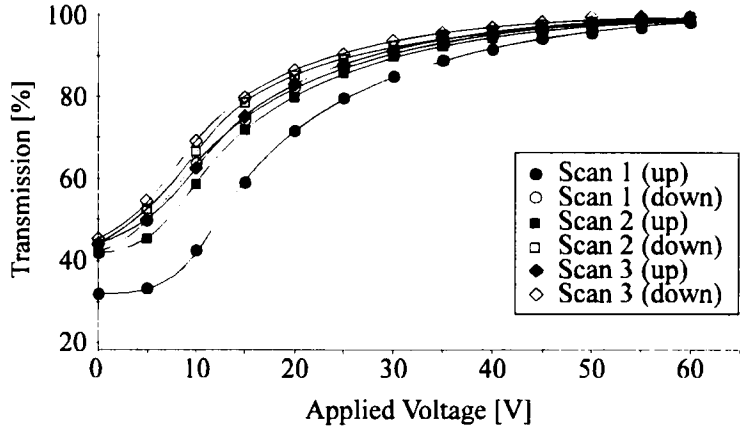

FIGURE 4 Electro-optic response of a 15μm thick PDLC film taken in repeated increasing and decreasing voltage scans (λ = 625 nm, ν = 140 Hz)

The electro-optic curves shown in Figure 4 are characterized by low threshold voltages and by high transmissions in the on-state. In addition of the observation of a well-known hysteresis phenomenon, it was also found that the PDLC film did not recover its scattering properties after the voltage scan cycles were completed. The transmission in the initial field-off-state was substantially lower as compared to the following off-states. Additionally, no change in the field-off transmission values was observed after completion of the first, second and third scan cycle. Several authors observed that PDLC films showing this electro-optic memory effect can be characterized generally by a polymer ball morphology, in which the liquid crystal droplets were large and irregularly shaped.[11,21,22] Further investigations will be necessary to clarify the relationship between the observed microdroplet morphology and the memory effect.

CONCLUSION

Well-defined PDLC films were obtained using EB radiation by a polymerization induced phase separation process. The electro-optic curves can be characterized by high transmissions in the on-state and by low threshold voltages. The transmission properties are strongly related to the effective refractive indices of the polymer matrix and the liquid crystal droplets. Monodisperse volume droplet size distributions were obtained from two

dimensional analysis of the PDLC films observed by SEM. Calculations of the microdroplet volume fraction and of the scattering cross sections have been performed. Further analysis of the PDLC materials is currently in progress.

ACKNOWLEDGEMENTS

The authors gratefully acknowledge the support of the C.N.R.S., the Région Nord-Pas de Calais and the Ministère de l'Enseignement Supérieur et de la Recherche. The authors are indebted to N. Gogibus, M. Kazic and A. Traisnel for their assistance.

REFERENCES

1. J.W. Doane in Liquid Crystals-Applications and Uses, edited by B. Bahadur (World Scientific, Singapore, 1990), Vol. 1, Chap. 14, pp. 361-395.
2. H.S. Kitzerow, Liq. Cryst., 16, 1 (1994).
3. N.A. Vaz, G.W. Smith, and G.P. Montgomery , Mol. Cryst. Liq. Cryst., 197, 83 (1991).
4. U. Maschke, X. Coqueret, and C. Loucheux, J. Appl. Polym. Sci., 56, 1547 (1995).
5. U. Maschke, X. Coqueret, and C. Loucheux, Nuc. Instr. Meth. Phys. Res. B, in press (1995).
6. N. A. Vaz, G.W. Smith, and G.P. Montgomery Jr, Mol. Cryst. Liq. Cryst., 146, 1 (1987).
7. a)Merck Liquid Crystals, Licrilite Brochure (1994); b) H.A. Tarry, The refractive Indices of Cyanobiphenyl Liquid Crystals, Merck Ltd, Great Britain (1967).
8. U. Maschke, X. Coqueret, M. Warenghem, M. Ismaili, unpublished results.
9. R. Havens, D.B. Leong, and K.B. Reimer, Mol.Cryst. Liq. Cryst., 178, 89 (1990).
10. C.H. Noh, J.E. Jung, J.Y. Kim, D.S. Sakong, and K.S. Choi, Mol. Cryst. Liq. Cryst, 237, 299 (1993).
11. F. G. Yamagishi, L. J. Miller, and C. I. van Ast, Proc. SPIE, 1080, 24 (1989).
12. R.T. DeHoff and F.N. Rhines, Trans. Met. Soc.AIME, 221, 975 (1961).
13. R.T. De Hoff, Trans. Met. Soc.AIME, 224, 474 (1962).
14. R.T. DeHoff, Quantitative Microstructural Analysis, Fifty years of progress in Metallographic techniques (ASTM STP 430, Am. Soc. Testing Mats., 1968), pp 63 - 95.
15. S.A. Saltykov, Stereometric Metallography, 2nd Edition (Metallurgizat, Moscow, 1958).
16. J.R. Kelly and P. Palffy-Muhoray, Mol. Cryst. Liq. Cryst., 243, 11 (1994).
17. N.A. Vaz and G.P. Montgomery Jr., J.Appl. Phys., 62, 3161 (1987).
18. D.K. Rout and S.C. Jain, Jpn. J. Appl. Phys; 30, 1412 (1991).
19. G.P. Montgomery Jr., N.A. Vaz, and G.W. Smith, Mol. Cryst. Liq. Cryst., 225, 131 (1993).
20. B.Bahadur, R.K. Sarna and V.G. Bhide, Mol. Cryst. Liq. Cryst., 72, 139 (1982).
21. R. Yamaguchi and S. Sato a) Jpn. J. Appl. Phys., 31, 254 (1992), b) Jpn. J. Appl. Phys., 30, 616 (1991).
22. R. Yamaguchi, H. Ookawara and S. Sato, Jpn. J. Appl. Phys., 31, 1093 (1992).